JOURNAL OF MATERIALS SCIENCE 21 (1986) 3467–3474

Transformation of $(Cr, M)_7C_3$-type carbides during nitriding of chromium alloyed steels

C. LEROY, H. MICHEL, M. GANTOIS
Laboratoire de Genie Metallurgique (UA CNRS 159-Science et Génie des Matériaux Métalliques)-Ecole des Mines, Parc de Saurupt, 54042 Nancy-Cedex, France

The *in situ* rearrangement of $(Cr, M)_7C_3$-type carbides has been observed during ion nitriding of a commercial chromium–carbon alloyed steel (Z160CDV12). The mass balance concerning nitrogen, carbon and substitutional elements proves that carbides undergo a total transformation into substitutional (Cr, M) N-type nitrides with a simultaneous release of α-iron from the very nitride phase. A detailed transmission electron microscopy microstructural study confirms the analytical results. There are no crystallographic relations between the carbides and their corresponding transformation products. The rejection of carbon from the carbides into the ferrite matrix leads to the precipitation of a network of cementite along the prior austenite grain boundaries.

1. Introduction

Nitriding allows for the formation of diffusion layers associated with phase transformations which induce large compressive stresses acting parallel to the plane of the specimen surface and modify tribological characteristics.

Such a treatment can be realized either in liquid or gas phase environments. In the latter case, the physical activation by means of an electric discharge produces surface layers more appropriate with respect to service performance [1, 2]. Metallurgical research in this field has led to a better understanding of the physical, chemical as well as the mechanical properties of such surface layers made up of γ' iron nitride and/or ε carbonitride [3–5].

The mechanisms of the structural hardening of the nitrided zones has been mainly studied in the case of binary systems, iron being associated to one of the following elements commonly found in steels: chromium, molybdenum, manganese, vanadium, silicon. . .[6]. For practical considerations, the system Fe–Cr is most interesting because of the great variety of surface properties that can be obtained this way. As a matter of fact, steels belonging to the system Fe–Cr–C are especially well suited for nitriding. In addition, their use is widespread, as chromium has a beneficial effect on the quenching speed of the bulk material and enhances carbide precipitation.

As a matter of fact, the structural hardening mechanisms encountered in binary alloys cannot be transposed directly to common commercially available chromium alloyed steels. This is due to the presence of carbon and various carbide phases. For example, it is a well established fact in metallurgy that diffusion layers in nitrided chromium alloyed steels contain a dense network of precipitates decorating prior austenite grain boundaries. For quite some time this phase was assumed to correspond to the precipitation of carbonitrides occurring in the course of nitriding [7, 8].

A structural and compositional analysis of ion-nitrided steels containing 5 to 12% has shown that in fact these networks are made up of cementite [9, 10]. The same findings have been published by Mridha and Jack [11] for 3% chromium-alloyed steel after gas phase nitriding. In general, for all chromium-alloyed steels, the carbon necessary for these kinds of precipitation results from a destabilization during nitriding either of primary or temper-induced M_3C, M_7C_3 and $M_{23}C_6$-type carbides. An *in situ* growth of CrN-type nitrides at the expense of temper-induced chromium carbides and/or alloyed cementite results of this rearrangement. It has been reported for various commercial steels [11, 12].

The main purpose of this paper is to present in detail the diffusional and structural mechanisms producing the transformation of $(Cr, M)_7C_3$-type carbides which can be analysed easily in a steel containing 12% Cr and 1.62% C first quenched and then tempered and nitrided at 540° C.

2. Experimental details

The steel studied here is a standard commercially available kind (AFNOR Z160CDV12) containing the elements (wt %) given in Table I.

Specimens were machined as parallelepipeds having the following dimensions: 25 mm × 10 mm × 40 mm. Prior to nitriding, they were subjected to the following heat treatment: austenizing for 25 min at 1080° C, quenching at 300° C, additional air cooling, tempering for 1 h at 570° C and additional tempering for 1 h at 540° C.

This treatment yields a very heterogeneous structure: primary as well as temper-induced $(Cr, M)_7C_3$-type carbides dispersed in a ferrite matrix with an overall hardness of 60 HRC.

0022–2461/86 $03.00 + .12

TABLE I Composition

C	Cr	Mo	Mn	V	Si
1.6	12	0.8	0.3	0.4	0.3

Nitriding is produced by means of ion bombardment. For the sake of easy observation and analysis of the diffusion layer, the specimens are kept for as much as 68 h in a N_2–H_2 atmosphere at 540° C which also yields a γ' compound surface layer. The overall gas throughout is 400 $cm^3 min^{-1}$, partial pressures being respectively 200 Pa for H_2 and 20 Pa for N_2.

Further to nitriding, for the purpose of metallography, part of the specimens are sectioned perpendicular to the nitrided surface and parallel to the major axes of the primary carbides.

Controlled etching in a nital solution (C_2H_5OH + 1.5% HNO_3) reveals most of the diffusion layer.

Radio-crystallographic examinations were done at different depths from the original surface by means of stepwise abrasion of layers of 10 μm in thickness (standard goniometer and Co$K\alpha_1$ radiation).

Transmission electron microscopy (TEM) as well as electron diffraction patterns were obtained from specimens sampled at different depths of the diffusion layer to allow for a detailed study of the various phase transformations. The thin foils for TEM were prepared by means of electrolytical thinning down followed by Ar-ion bombardment induced sputtering. TEM was done with a Jeol 200CX at 200 kV.

By means of quantitiative electron microprobe and associated X-ray images, the distribution of metallic elements as well as interstitial non-metallic components could be tracked within the nitrided layers.

The following reference standards have been retained to allow for such quantitative measurements:

1. Diamond, cementite and (Cr, M)$_7C_3$-type carbides (8.7 ± 0.2 wt % C) for the carbon content in the primary carbides.
2. Fe–C alloys of well-known chemical composition for the carbon content in the base matrix.
3. A 5 μm layer of γ' Fe_4N on a bulk specimen of pure iron for N_2 content.
4. Pure metal standards for quantitative analysis of the metallic elements.

3. Experimental results and discussion

3.1. Micrographical observations

Within the nitrided layer (Fig. 1) chemical etching reveals three distinct sublayers:

Zone I: a 110 μm thick surface sublayer where primary carbides do not seem to be affected by the treatment,

Zone II: an 80 μm intermediate sublayer with a characteristic, dense network of filiform precipitates,

Zone III: a 50 μm transition sublayer with a continuous change from the nitrided structure to the base material.

Except for the primary carbides one might expect an analogous situation for any nitrided chromium-alloyed steels. However, these observations do not characterize the very structure of the diffusion layer as investigated by means of X-ray diffraction and electron microprobe analysis.

3.2. X-ray diffraction analysis

The non-nitrided steel is characterized by ferrite and (Cr, M)$_7C_3$-specific diffraction patterns. Next to the nitrided surface (zone I), one observes in addition to ferrite and γ' diffraction lines those of another phase with fcc structure and a lattice parameter a_0 = 0.415 nm as expected for CrN.

At 140 μm below the surface, within zone II, cementite diffraction lines are superimposed to those originating from chromium nitride and ferrite. We shall consider them to be due to the precipitate network observed at this very level.

Up to this depth, no (Cr, M)$_7C_3$-type diffraction lines can be resolved. They only exist close to the diffusion front (zone III) coinciding with the depth dependent intensity decrease of the CrN-specific diffraction lines.

3.3. Electron microprobe analysis

All of the X-ray images (carbon, nitrogen, iron, chromium) sampled over the 100 μm sublayer close to the surface yield evidence during the nitriding process of nitrogen substituting carbon on sites formerly occupied by primary carbides of the zones I and II (Fig. 2).

Cementite formation in zone II should therefore be attributed to carbon left over when carbides are transformed into nitrides.

At the matrix-diffusion layer interface, images of backscattered electrons as well as carbon and nitrogen specific X-rays allow for an observation of the different stages of this mechanism (Fig. 3).

For the primary carbides, one observes a contrast between the zones where transformation is progressing or else entirely complete. This should be taken as evidence that the transformation proceeds according to an interface displacement mechanism. At the same time, at a submicroscopic level there is a reorganization but the original image of the carbide is preserved, temperature being insufficient to allow for metallic diffusion over a distance of more than a few lattice parameters.

A quantitative analytical balance covering all interstitial and substitutional elements has been done for the following experimental situations: non-nitrided base matrix, (Cr, M)$_7C_3$-type carbides, nitrided matrix and converted carbides.

The corresponding results are compiled in Table II.

The initial carbon concentrations (wt %) are close to 0.8% in the non-nitrided base matrix and 8.7% for the primary carbides. This distribution is considerably modified in the nitrided zone with an overall variation from 0 to 0.8% C when starting from the surface and proceeding down to the diffusion front. The underlying mechanism, already observed with lower chromium alloyed steels [10, 11, 13] is valid for nitriding of any chromium-alloyed steel.

Within the converted carbides, the carbon content is zero which confirms the fact of a complete expulsion of this element towards the ferrite matrix. This is true

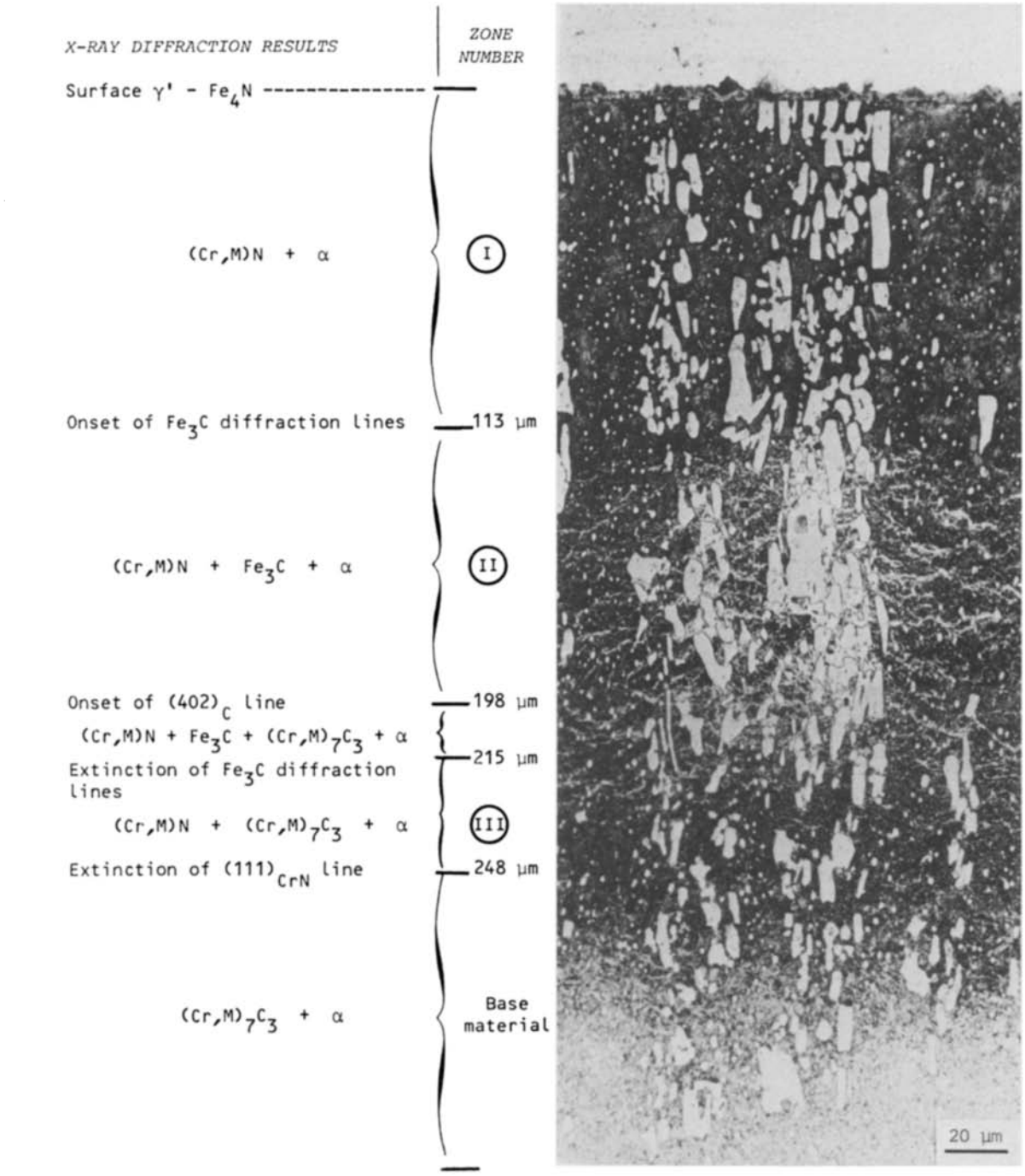

Figure 1 12% Cr steel, Z160CDV12 ion nitrided for 68 h at 540° C. (a) Transverse optical micrograph; specimen etched in nital (1.5%); (b) X-ray diffraction results from successives depths of diffusion zone.

even during the transformation process of primary carbides, a fraction of which coexists together with the newly formed nitrides. As a matter of fact in this situation the only carbon detected is chemically bound in the very residual fraction of non-converted primary carbides.

The distribution of the metallic alloying elements is essentially unaffected by the nitriding process. This explains why the original contours of the primary carbides are unaffected during nitriding. However, this does not preclude a possible substitution within the nitride precipitates.

Quantitative analysis of the primary carbides yields $Cr_{3.62}M_{3.38}C_3$ which corresponds to practically stoichiometric carbide with a ratio Cr/M close to unity. This result agrees with the work published by Benz *et al.* [14] who showed that in case of Cr_7C_3 other metal elements like vanadium and molybdenum can be continuously substituted for chromium without modifying the overall stoichiometry of the carbide.

Considering that the structural transformation of monocrystalline carbides consists of a simple substitution of nitrogen for carbon accompanied by some local rearrangement of all of the metal atoms, the overall chemical formula obtained from the above analysis would be $(Cr_{0.76}, M_{0.59})N$. As such non-stoichiometry does not seem compatible with a nitride having CrN structure, we have checked whether there is really simple substitution of the metallic elements in the carbide towards the corresponding nitride. In order to get such an experimental check, we have nitrided for 50 h (Cr, Fe, $V)_{6.9}C_3$-type carbides

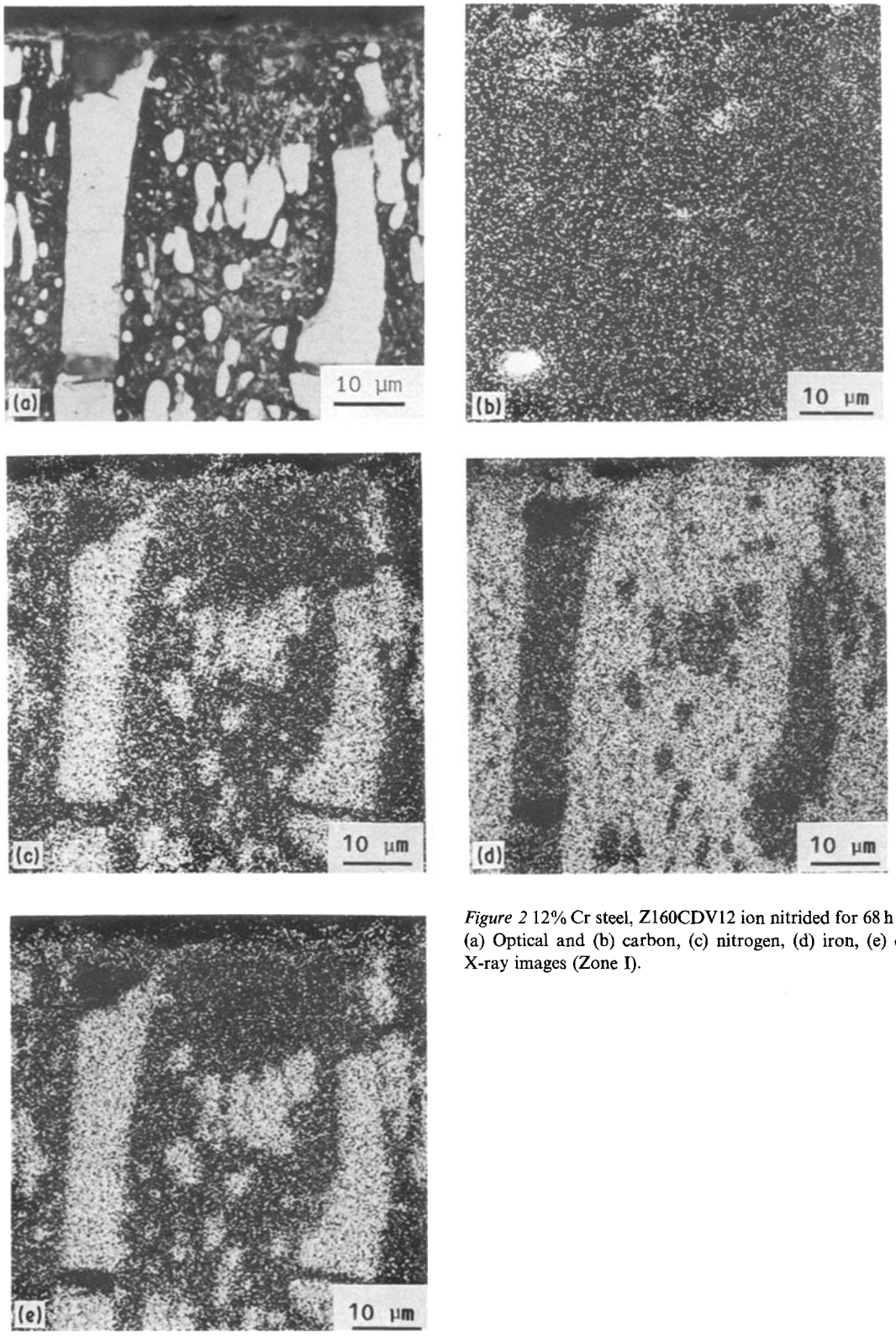

Figure 2 12% Cr steel, Z160CDV12 ion nitrided for 68 h at 540° C. (a) Optical and (b) carbon, (c) nitrogen, (d) iron, (e) chromium X-ray images (Zone I).

TABLE II 12% Cr steel, Z160CDV12 ion nitrided for 68 h at 540° C. Non-nitrided base matrix, $(Cr, M)_7C_3$ primary carbides, nitrided base matrix and converted $(Cr, M)_7C_3$ carbides quantitative microanalysis results

Elements	Content: wt% (at %)			
	(Cr, M) N	Nitrided base matrix	$(Cr, M)_7C_3$	Non-nitrided matrix
C	0 (0)	0 (0)	8.7 ± 0.3 (30 ± 1)	0.77 ± 0.05 (3.35 ± 0.22)
N	16.6 ± 0.5 (42.4 ± 1.2)	2.8 ± 0.1 (9.9 ± 0.3)	0 (0)	0 (0)
Fe	29.6 ± 0.4 (18.9 ± 0.3)	87.7 ± 0.3 (78.2 ± 0.3)	35.6 ± 0.2 (26.3 ± 0.2)	90.0 ± 0.5 (84.3 ± 0.5)
Cr	47.2 ± 0.8 (32.4 ± 0.6)	8.2 ± 0.2 (7.8 ± 0.2)	45.5 ± 0.4 (36.2 ± 0.3)	7.9 ± 0.2 (8.0 ± 0.2)
Mo	2.48 ± 0.05 (0.92 ± 0.02)	0.61 ± 0.05 (0.32 ± 0.03)	3.4 ± 0.2 (1.46 ± 0.08)	0.70 ± 0.05 (0.38 ± 0.03)
V	5.6 ± 0.1 (3.9 ± 0.1)	0.35 ± 0.05 (0.34 ± 0.05)	5.5 ± 0.1 (4.5 ± 0.1)	0.33 ± 0.02 (0.34 ± 0.02)
Mn	0.70 ± 0.03 (0.45 ± 0.02)	0.51 ± 0.02 (0.46 ± 0.02)	0.67 ± 0.02 (0.50 ± 0.02)	0.52 ± 0.02 (0.49 ± 0.02)
Si	0.75 ± 0.05 (0.95 ± 0.06)	1.7 ± 0.05 (3.0 ± 0.1)	0.70 ± 0.05 (1.04 ± 0.06)	1.69 ± 0.04 (3.1. ± 0.1)

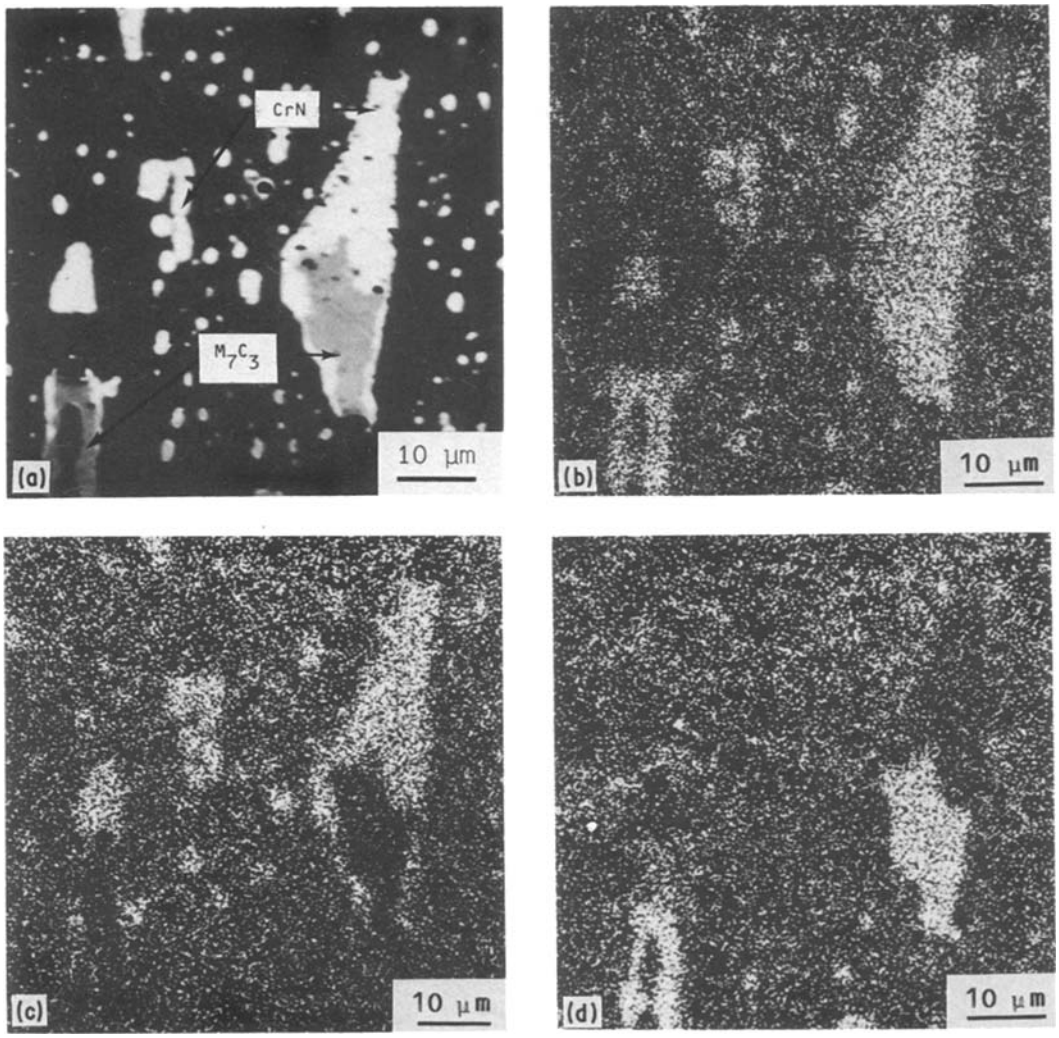

Figure 3 12% Cr steel, Z160CDV12 ion nitrided for 68 h at 540° C. (a) Electronic and (b) chromium, (c) nitrogen, (d) carbon X-ray images (Zone III).

extracted from chromium-alloyed white cast iron. The X-ray analysis done after this treatment clearly shows that, in reality, there is simultaneous formation of ferrite and nitride (Tables III and IV). On account of these results and considering that iron in the nitride obtained is not substituted for chromium, in addition to the low solubility of nitrogen in α-iron, the chemical composition should be $(Cr_{0.76}, M_{0.15})N$ which approaches stoichiometry.

The mass balance done for the region of complete decarburization of the nitrided matrix (30 μm below the surface) reveals that once more, nitrogen occurs chemically bound as CrN-type nitrides.

These nitrides are the products of two mechanisms: direct precipitation from alloying solid solution elements within the ferrite as well as temper-induced carbide rearrangement identical with that of the primary carbides.

A more detailed study of these transformations has been done by means of TEM.

TABLE III M_7C_3 carbides chemically extracted from chromium-alloyed white iron, then nitrided 50 h at 540° C. Theoretical and experimental X-ray diffraction analysis results

(*h k l*)	*d* spacing (nm)		
	Theoretical results	Experimental results	
		Before nitriding	After nitriding
(4 0 1) M_7C_3	0.2515	0.252_4	0.251_8
(1 1 1) CrN	0.2395	–	0.239_3
(4 1 1) M_7C_3	0.2281	0.228_5	0.228_5
(4 2 0) M_7C_3	0.2288	0.228_5	0.228_5
(2 0 2) M_7C_3	0.2118	0.210_6	0.210_3
(2 0 0) CrN	0.2074	–	0.207_4
(4 2 1) M_7C_3	0.2041	0.203_7	0.204
(1 1 0) α	0.2026	–	0.202_6
(6 0 0) M_7C_3	0.2017	0.201_7	0.201
(6 0 1) M_7C_3	0.1842	0.183_9	–
(4 0 2) M_7C_3	0.1811	0.180_5	–
(3 2 2) M_7C_3	0.1753	0.174_5	0.174_6
(4 4 0) M_7C_3	0.1747	0.174_5	0.174_6
(2 2 0) CrN	0.1467	–	0.146_4
(2 0 0) α	0.1433	–	0.143_1

3.4. TEM observations

3.4.1. Structural transformation of primary carbides

TEM shows that the $(Cr, M)_7C_3$-type carbide crystals

TABLE IV Carbide, nitride and ferrite lattice parameters calculated from Table III results

Phase	Structure	Parameters (nm)
α	cc	$a = 0.2867 \pm 0.0005$
$(Cr, M)_7C_3$	hexagonal	$a = 0.1397 \pm 0.002$ $c = 0.448 \pm 0.004$
(Cr, M) N	fcc	$a = 0.4145 \pm 0.0005$

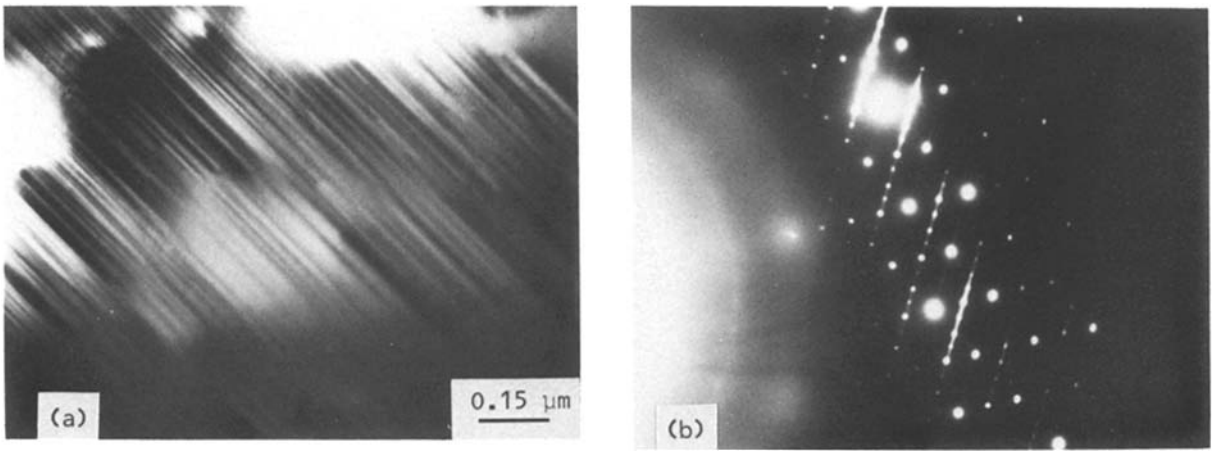

Figure 4 (a) TEM (Cr, M)$_7$C$_3$ primary carbide microstructure. (b) Corresponding electron microdiffraction pattern: first-order Laue-zone with a small section of the $(0\,0\,0\,1)^*_{hex}$ planes showing two families of streaks parallel to the $\langle 1\,\bar{1}\,0\,0\rangle^*$ directions. Punctuated streaks indicate a four plane stacking fault periodicity.

contain an important amount of planar defects [15] (Fig. 4). Studying the first order Laue zone from (M, Cr)$_7$C$_3$ carbides on a crystal with *c*-axis aligned parallel to the direction of the electron beam, it can be shown that the unit cell of these carbides is orthorhombic as suggested by Fruchart and Roualt [16].

The assessment of the structure and morphology of nitrides in the region of carbide to nitride rearrangement has been done on appropriately thinned down foils sampled at different depths of the nitrided layer.

Within the carbide to nitride transition zone, the rearrangement inside of a carbide crystal proceeds via progressive displacement of an abrupt growth front interface (Fig. 5).

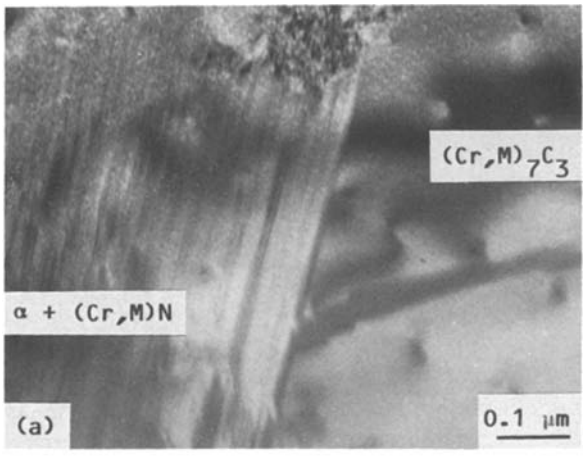

The planar defect systems do not seem to favour preferential diffusion of interstitial elements.

The growth front specific electron diffraction patterns do not reveal any particular crystallographic relations between the carbide and its corresponding transformation products: (Cr, M)N and α-iron (Fig. 5b).

Finally, as opposed to the assumption of Jonck and Kunze [17], we did not observe any intermediate carbonitride phases.

Microdiffraction analysis reveals a pseudo-fibrous texture for the nitride crystals, each of them having a diameter of about 10 nm.

Close to the surface, where total conversion takes place, a volume initially occupied by a (Cr, M)$_7$C$_3$ single crystal takes up a microcrystalline, mixed structure of f c c (Cr, M)N and finely dispersed b c c ferrite crystals with a well defined boundary with respect to ferrite base matrix (Fig. 6). These results are in excellent agreement with the former analytical results.

Figure 5 (a) Bright-field micrograph showing a carbide to converted carbide transition zone (Zone III); (b) electron-diffraction pattern of the transition area; (c) key to the electron diffraction pattern. $[0\,0\,0\,1]_{(Cr,M)_7C_3}$ Laue-zone, α and (Cr, M)N specific diffraction patterns.

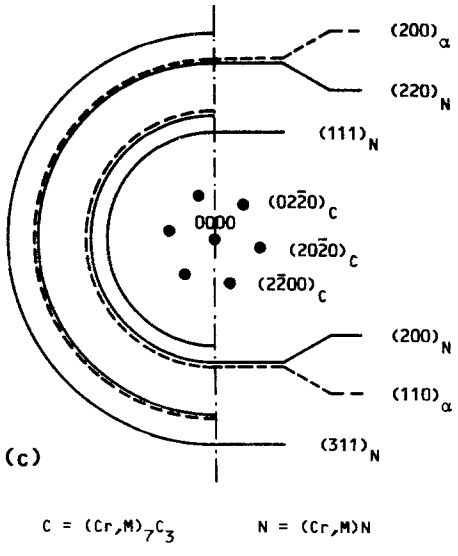

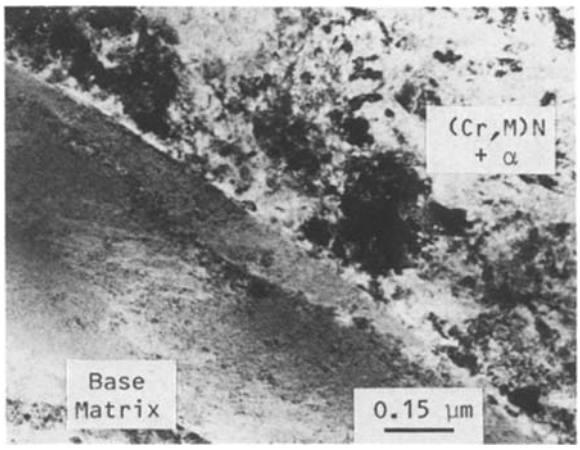

Figure 6 Bright-field micrograph showing the interface transition between base matrix and converted primary carbide (Zone I).

Repeated tempering of the steel studied here produces considerable precipitation of finely dispersed (Cr, M)$_7$C$_3$-type carbides. Microtwins and prior martensite lath boundaries are preferential sites for nucleation and growth of these carbides. In a way analogous to the transformation process described for primary carbides, nitriding produces *in situ* conversion of temper-induced carbides into CrN-type nitrides and ferrite. This feature is shared by all chromium-alloyed steels including the case when the temper-induced carbides are composed of alloyed cementite [11].

3.4.2. Cementite precipitation

TEM studies of thin foils from the carbon-rich zone of the nitrided layer confirm the presence of cementite originally detected by means of X-ray diffraction.

Cementite precipitation starts from carbon saturated ferrite yielding either large areas of extremely fine crystals or else a multitude of isolated islets (Fig. 7). Nucleation normally occurs in ferrite along the prior austenite grain boundaries, growth proceeding according to the well-known Bagaryatskii mechanism [18].

3.4.3. Structural hardening of the nitrided layer

The CrN phase which replaces chromium carbides is too coarse in order to contribute to the hardening of the nitrided layer.

During nitriding, prior to the phase transformations discussed above, there is a preliminary stage when CrN-type nitrides, coherent with the ferrite matrix, precipitate according to special crystallographic orientations [19, 20]. They give rise to the surface hardening observed experimentally. As for binary Fe–Cr alloys, the nucleation sites are located at the $\{1\,0\,0\}_\alpha$ faces of the α solid solution crystals. At the very diffusion front, they produce diffraction patterns of somewhat diffuse intensity along $\langle 1\,0\,0\rangle^*_\alpha$ equivalent directions.

The density of these CrN-type precipitates and thus the average hardness of the nitrided layer will depend on the fractions of chromium and other alloying elements present in the carbides and the matrix base material once the heat treatment of the steel is completed.

4. Conclusions

A mass balance concerning nitrogen, carbon and substitutional alloying elements has been done for the nitrided layers of Z160CDV12 steel. This mass balance proves that primary (Cr, M)$_7$C$_3$-type carbides undergo an *in situ* rearrangement into substitutional (Cr, M) N-type nitrides with a simultaneous release of α-iron from the very nitride phase. There is no correlated apparent morphological evolution occuring. The original images of the primary carbides are preserved.

A detailed TEM microstructural study has confirmed within the transmuted primary carbides the presence of polycrystalline compound structures containing ferrite and nitrides.

There are no crystallographic relations between the carbide and its corresponding transformation products. The temper-induced carbides will obey the same mechanisms.

This study confirms that following the rejection of carbon from the carbides, there is formation of cementite spreading within the ferrite matrix and forming a network of precipitates specially along the prior austenite grain boundaries.

References

1. G. HISLER, D. GERARDIN, H. MICHEL and M. GANTOIS, *Traitement Thermique* **140** (1979) 63.

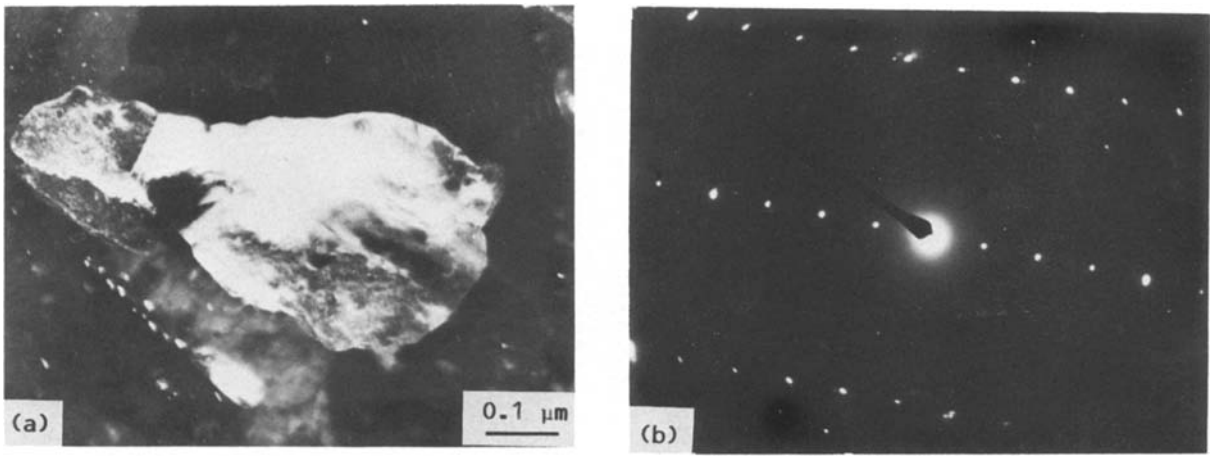

Figure 7 (a) Dark-field electron micrograph of a cementite islet obtained with the $(0\,0\,1)_{Fe_3C}$ diffracted beam; (b) electron diffraction pattern of the same area. $[\bar{1}\,\bar{1}\,3]_\alpha$ and $[2\,\bar{1}\,0]_{Fe_3C}$ Laue-zones.

2. J. P. PEYRE and A. DUBUS, in Proceedings of the 18th International Conference on Heat Treatment of Materials, Detroit, Michigan USA, 6–8 May 1980 (ASM, Metals Park, Ohio) p. 312.
3. D. GERARDIN, H. MICHEL and M. GANTOIS, *Scripta Metall.* **11** (1977) 557.
4. D. GERARDIN, J. P. MORNIROLI, H. MICHEL and M. GANTOIS, *J. Mater. Sci.* **16** (1981) 159.
5. M. EL HAJJAJI, M. FOOS, H. MICHEL and M. GANTOIS, *Scripta Metall.* **17** (1983) 879.
6. K. H. JACK, in Proceedings of the Heat Treatment'73 Conference, London, December 1973 (The Metals Society, London, 1975) p. 39.
7. T. LYMAN (ed), "Metals Handbook", (ASM, Metals Park, Ohio, USA, 1972).
8. B. EDENHOFER, *Heat Treat. Met.* **1** (1974) 59.
9. C. LEROY, H. MICHEL and M. GANTOIS, in Proceedings of the 2nd International Conference on Heat Treatment of Materials of IFHT, Florence, September (1982) p. 207.
10. C. LEROY, INPL thesis, Nancy (1983).
11. S. MRHIDA and D. H. JACK, *Met. Sci.* **16** (1982) 398.
12. B. J. LIGHTFOOT and D. H. JACK, in Proceedings of the Heat Treatment'73 Conference, London, December 1973 (The Metals Society, London, 1975) p. 59.
13. A. M. MINKEVIC and Y. V. SOROKIN, *Härt. Tech. Mitt.* **25** (1970) 108.
14. R. BENZ, J. F. ELLIOT and J. CHIPMAN, *Metall. Trans.* **5** (1974) 2235.
15. J. P. MORNIROLI, E. BAUER-GROSSE and M. GANTOIS, *Phil. Mag. A* **48** (1983) 31.
16. R. FRUCHART and A. ROUALT, *Ann. Chim.* **4** (1969) 143.
17. R. JONCK and G. KUNZE, *ZwF 73* **4** (1978) 213.
18. YU. A. BAGARYATSKII, *Dokl. Akad. Nauk. SSSR* **73** (1950) 1161.
19. R. G. BACKER and J. NUTTING, *ISI Special Report* (1959) 64.
20. B. MORTIMER, P. GRIEVESON and K. H. JACK, *Scand. J. Metall.* **1** (1972) 203.

Received 16 October
and accepted 25 November 1985